

PVD Coating of Mg–AZ31 by Thin Layer of Al and Al–Si

Mohamed A. Taha, Nahed A. El-Mahallawy,
Rawia M. Hammouda, Sherif I. Nassef

© FSCT and OCCA 2010

Abstract Although magnesium alloys have the advantage of high specific strength, they have poor atmospheric corrosion resistance. An important method of improving the corrosion resistance is by applying a coating layer. In this work, the physical vapor deposition (PVD) technique is used for coating a magnesium (Mg) AZ31 sheet substrate with a thin layer of high purity aluminum (Al) and Al–12.6% Si. Aluminum is expected to be suitable as a coating layer on Mg sheets, due to its corrosion resistance and its formability. Before coating, the substrate was subjected to several consecutive surface preparations, including sand-blasting, mechanical grinding, mirror-like polishing, ultrasonic etching, and finally ion etching by magnetron sputtering (MS). PVD coating was conducted using a PVD machine with max electron beam power and voltage of 100 kW and 40 kV, respectively. This was either with or without plasma activation, and with variable substrate speeds ranging between 10 and 70 mm/s. During MS ion etching and coating, the substrate temperature increased. The substrate temperature increased with the application of plasma activation and with lower substrate speeds. The coating-layer thickness varied inversely with substrate speed. A thinner coat with finer morphology was obtained in the case of plasma activation. Other results included coating layer characteristics, diffusion between the AZ 31 substrate and the Al coating layer, adhesion of the coating layer to the substrate, and corrosion resistance by a humidity test.

Keywords Mg AZ31B, PVD coating, MS ion etching, Diffusion, SEM and GDEOS, Adhesion, Corrosion

M. A. Taha (✉), N. A. El-Mahallawy,
R. M. Hammouda, S. I. Nassef
Faculty of Engineering, Ain-Shams University, Cairo, Egypt
e-mail: m_ataha@yahoo.com

Introduction

Magnesium alloys are the lightest alloys, with about two-thirds (2/3) the density of aluminum. They have high modulus and excellent antishock resistance. This makes them attractive for several industrial applications where light weight and good strength are required. The heat conductivity and electromagnetic shielding effectiveness are also added to the advantages of magnesium alloys for the information technology and communication industries.^{1–3} One drawback, however, is that they are prone to atmospheric corrosion. Because of their high chemical affinity to aqueous solutions, they are difficult metals for electrochemical treatments. Magnesium quickly forms a very thick oxide layer that varies between 0.2 and 0.25 μm , in comparison with the oxide layer on steel that equals approximately 10 nm.

Different surface treatment techniques and coatings for magnesium and its alloys are found in the literature, either for decorative or functional purposes. The advantage of the application of metallic coatings on magnesium surfaces is that they provide a corrosion resistance in addition to a conductive, high temperature-resistant, hard, reflective, and solderable surface.^{4–11} A review of the different methods for coating Mg surfaces can be found elsewhere.⁴ Surface treatment by coating is among the most commonly used treatments, including chemical inorganic coating, inorganic conversion coating, and anodizing (e.g., chromating fluorozirconate treatment), organic, metallic, ceramic coating, as well as composite coatings.¹² Direct electroplating is difficult to apply to magnesium, however, due to the high reactivity of the substrate with aqueous solutions.⁴ The electroless technique for coating with an Ni–P layer is among the recent methods for the surface protection of Mg alloys.^{4–6,13} Among the surface treatment techniques for improving the corrosion resistance of Mg alloys are vapor deposition,⁷

coating with an oxide layer,⁸ sol gel coating,⁹ and the thermal spray of different alloys.¹⁰

The Al–12% Si alloy was deposited by plasma spraying on an Mg AS41/carbon short fiber composite, then remelted using a CO₂-laser beam (laser clad).¹⁴ The process parameters have to be very restricted, however, to prevent the temperature rise of the Mg surface and porosity formation after laser remelting.

The application of aluminum coating on AZ31 alloy was achieved by arc spray coating followed by a post-treatment consisting of hot pressing to reduce the amount of pores present in the coating layer. Then a final anodizing treatment is applied.¹⁵ This treatment remarkably improved the corrosion resistance of the alloy in a sodium chloride (NaCl) solution, but the process is dependant on the geometry of the component for the pressure application step.¹⁵

The thermal spray of Al–5% Si using arc spray coating was investigated with a pre- and post-heat treatment,¹⁶ but the coat was found to include very high porosity. Sealing with epoxy or polyurethane was therefore necessary. Another technique using high velocity oxy-fuel sprayed NiCr, and NiCr-chromium carbide coating was found to adhere well to the substrate. The presence of microporosity, however, caused severe corrosion at the interface between the coat and substrate.¹⁶

The protection of magnesium surfaces still represents an attractive research topic, as there is a need to enhance the corrosion resistance of Mg alloys through optimizing coating methods and procedures.¹²

In the present work, we studied the coating of Mg AZ31 sheet substrates with pure Al and Al–12.6% Si alloy layers. Aluminum has good corrosion resistance and is also deformable. Therefore, it is expected to be suitable for coating Mg sheets, which can be shaped after coating. The physical vapor deposition (PVD) technique is used, as it is a promising technique for coating sheets.¹⁷

Experimental work

The substrate used in the present work is AZ–31 (3% Al, 1% Zn, and 0.2% Mn). The sample size is 120 mm × 200 mm × 1.6 mm thick. The coating material was either high purity Al (99.99%) or high purity Al–12.6% Si alloy.

Coating procedures include initial substrate surface preparation followed by PVD coating. The PVD machine used was an EMO machine [max electron beam (EB) power and voltage were 100 kW and 40 kV, respectively]. A separate lock vacuum chamber, in which MS ion etching took place, was attached to the PVD machine. Both the etching chamber and machine coating represented a sealed system, in which the lock was opened after etching to let the sample substrate move under vacuum to the coating chamber.

The first step for substrate pretreatment prior to coating was the surface mechanical preparation by sand blasting, grinding and polishing. Ultrasonic cleaning was then conducted in a solution of sodium carbonate (Na₂CO₃) 25 g/L and sodium hydroxide (NaOH) 15 g/L at 65°C for 3 min, followed by water rinsing.¹⁸

Before ion etching and coating, a thermocouple was welded to the substrate sample to record its thermal history during coating. The sample was then put inside the lock vacuum etching chamber. After evacuation to a pressure of 10^{–5} mbars, ion etching was conducted. An electric discharge occurred between the substrate sample (cathode) and the etching vacuum chamber (anode) in the presence of argon gas. Two ion-etching methods were investigated, namely glow discharge (GD) etching, and magnetron sputtering (MS). Meanwhile, EB conditioning of the aluminum bath (target material) was done for 3 min.

The next step was coating inside the PVD vacuum chamber, where evaporation of the coating material was achieved by EB, which was the source of energy and was created by an electron gun. Coating stroke was applied by moving the substrate over the evaporating molten pool. Different experiments with different substrate speeds were investigated. After coating, the specimen was left inside the PVD vacuum chamber for cooling to 100°C. After cooling, the sample was removed from the vacuum chamber and weighed. The layer thickness was calculated from the difference in weights before and after coating.

Coating characterization was completed for layer thickness, surface morphology, diffusion of the coating material into the substrate using GD for emission of spectrum (GDEOS), microhardness, adhesion using a tape test before and after bending, and corrosion resistance using a humidity test.

Results and discussion

Substrate surface pretreatment and ion etching

The main objective of substrate surface preparation is to remove the thick oxide layer that usually forms rapidly on Mg surfaces and prevents successful coating.^{13,17,19} In preliminary experiments, mechanical pretreatment was applied prior to ion etching. Different procedures were conducted as combinations of grinding, sand-blasting, polishing, and polishing to a mirror-like surface. The procedures involving sand-blasting and final polishing up to a mirror-like surface proved to be optimum as a first step prior to ion etching.

The mechanical pretreatment was followed by ion etching, which represented an essential step in Mg surface preparation before coating.^{18,20} The bombardment of argon atoms on the substrate resulted in the removal of nanoparticles or fine oxides and was

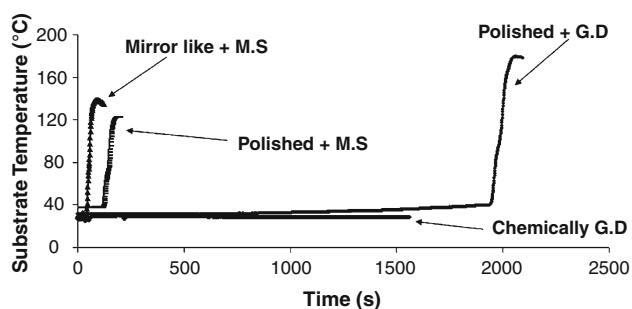


Fig. 1: Variation of Mg AZ 31 substrate temperature with etching time, using different MS and GD ion etching and different mechanical and chemical pretreatment methods

responsible for activating the surface and enhancing adhesion between the substrate and coating.^{18,20}

In a group of experiments for optimizing the ion-etching procedure, the temperature of the substrate was monitored. It was found that during ion-etching, the substrate temperature increased, as shown in Fig. 1. The heating time and the maximum temperature reached depended on the procedures applied. Figure 1 shows that in the case of MS ion etching, the substrate temperature increased within 100 s to a maximum of 140°C (substrate polished to mirror-like surface) and within 200 s to a maximum of 120°C (substrate roughly polished). In the case of GD ion etching, a much longer time of 2000 s (10 times) was needed to reach a maximum temperature of 180°C (substrate rough polished).

Substrate heating during ion etching was due to the argon atoms' bombardment of the substrate surface, which was retarded by the oxide layer. The heating time was taken as an index for the rate of oxide removal. Accordingly, in case of MS, the shorter heating time and lower maximum temperature, in comparison to GD, was taken as an indication that MS is more efficient in removing the oxide layer. In the literature,¹⁷ GD was used successfully in the case of steel sheets, which usually have a much thinner oxide layer. The same reference reported that MS is suggested for the case of substrate alloys with a thick oxide layer.

From the preliminary experiments, MS ion etching is considered effective in removing the oxide layer from the AZ31 surface. The optimum surface preparation procedures include sand-blasting, mirror-like polishing, and ultrasonic cleaning followed by MS ion etching, which will be used for the following coating experiments.

PVD coating process

In this work, PVD coating was conducted using Al and Al–12.6% Si alloy substrates with optimum surface preparation, either with or without plasma activation. Plasma activation was conducted using a separate device for hollow cathode arc-activated deposition

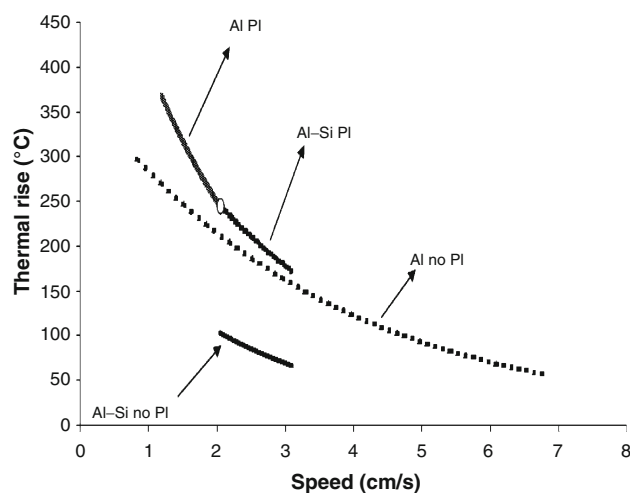


Fig. 2: Variation of thermal increases during PVD coating with substrate speeds for samples coated with Al or Al–12.6% Si alloy, with plasma (PI) or without plasma (no PI)

which was attached to the PVD machine. The substrate speed was varied to study its effect on the coat.

During PVD coating, the substrate was found to be additionally heated, as indicated in Fig. 2. In PVD coating, most of the beam energy is used to heat up and vaporize the coating material. As a result, the vapor stream condenses on the substrate surface and loses most of the energy as the heat of condensation, thus providing a thermal load on the substrate.^{17–19}

Figure 2 indicates the temperature rise measured for several specimens coated with different substrate speeds and under different conditions. Such conditions include cases of Al or Al–12.6% Si, either with or without plasma activation. The results show that the temperature increase value is inversely proportional to the substrate speed. This can be explained as: lower substrate speed means that the substrate surface has been exposed to the condensed vapor stream for a longer period of time.

The results in Fig. 2 indicate that pure Al resulted in a higher temperature increase than Al–12.6% Si, for plasma or no plasma activation. This can be attributed to the different thermal properties of the materials.

The use of plasma activation resulted in a larger temperature increase in the substrate, compared to the case of no plasma activation. Plasma activation is a source of extra energy provided to the deposited atoms that heats the vapor stream more.^{17,18} It was used in a previous work¹⁷ on steel substrates to provide sufficient energy for structure rearrangement, thus obtaining a dense coat layer instead of a columnar porous structure.

Coating layer thickness

The thickness of the deposited layer was calculated from the weight gain of the substrate after coating.

Figure 3 shows that coat thickness is generally inversely proportional to the substrate speed. This can be explained by lower substrate speed, which means that the substrate surface has been exposed to the condensed Al (or Al–12.6% Si) vapor stream for a longer period of time.

Figure 3 shows that Al and Al–12.6% Si coatings at the same substrate speed obtained a much thicker layer with no plasma activation in comparison to those with plasma activation. This can be explained by the fact that plasma activation results in EB dispersion during deposition, which in turn leads to a decrease in the density of the vapor stream coming out from the target material.¹³ Thus the deposition rate decreases and the coating layer is thin. The difference in coat thickness is remarkable at lower substrate speeds, while both thickness values tend to be close to each other at higher speeds, which is attributed to the difference in exposure time.

A static deposition rate can be defined as the rate of layer deposition if the specimen is not moving (zero passing speed). It is calculated by dividing the layer's thickness by the time of coating, which was automatically recorded by the machine. Figure 4 presents the calculated static deposition rate for the samples with different conditions and different target materials. A higher static deposition rate was found in the case of the Al target, compared to the Al–12.6% Si target.

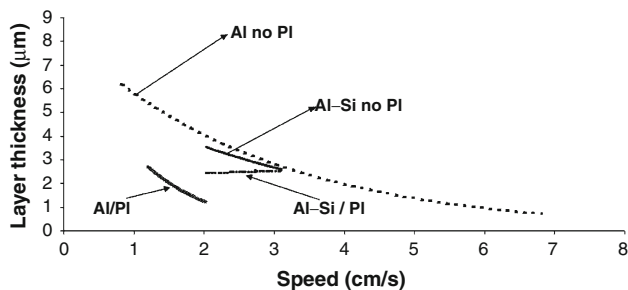


Fig. 3: Influence of substrate speeds on layer thickness applying different coating conditions; with plasma (PI) and without plasma (no PI)—coating by Al or Al–12.6% Si alloy

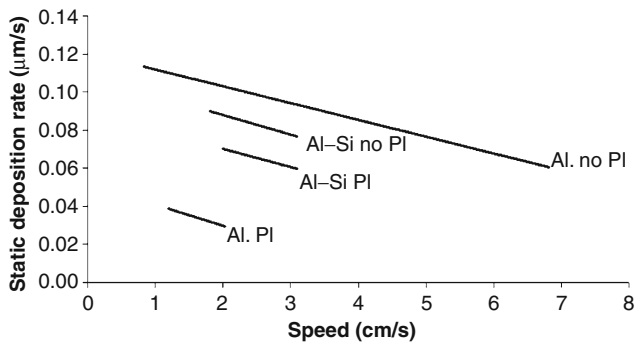


Fig. 4: Variation of static deposition rate, with substrate speed: plasma (PI) and without plasma (no PI)—coating by Al or Al–12.6% Si alloy

In the case of the Al–Si target, the thickness of the coating layer remained almost constant with varying substrate speed, and the influence of plasma was not very pronounced as compared to the Al target, as shown in Fig. 3. This was attributed to the difference in vapor pressures between Al and Si,¹³ which results in a decrease of the beam power during deposition (beam power recorded ranged between 20 and 40 kW in the case of the Al–Si target, and between 80 and 100 kW in the case of the Al target).

The data on thermal increases and coating thicknesses are presented again in Fig. 5. The figure describes the variation of layer thickness and substrate temperature with processing time, thus describing the whole process history, including ion etching and coating. The data presented are for two typical samples with similar surface preparation conditions and MS ion etching, target material (Al) and MS-coating conditions, and speed, but one with plasma activation and one without. During the etching period of 180 s, the substrate was heated to 150°C. During the following coating period of 100 s, the substrate continued to heat up, reaching 400°C in the case of no plasma activation, while it was only slightly higher at 450°C in the case of plasma activation. However, Fig. 5a indicates a layer thickness of 3 µm in the case of plasma activation, while it doubled to 6 µm in the case of no plasma activation. As in both cases, because the substrate temperatures are relatively close, the reduction of layer thickness in the case of plasma activation can be due to EB dispersion, as mentioned previously.

Coating layer morphology

The coating layer followed the same surface profile that resulted from surface preparation. This is

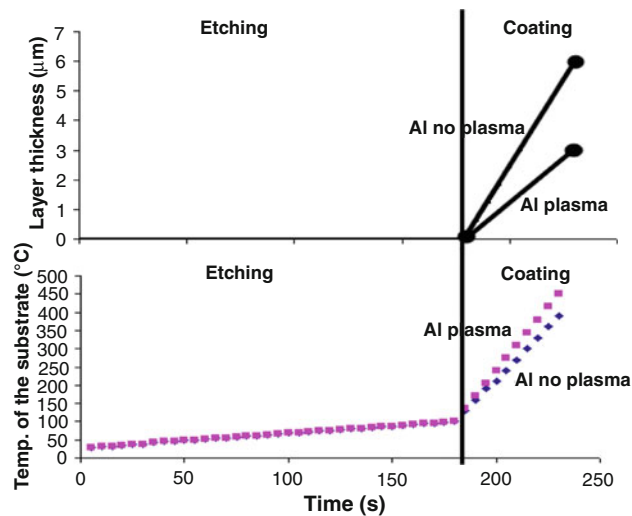


Fig. 5: Variation of: (a) coat layer thickness; (b) substrate temperature during the processing history for typical coating experiments with and without plasma, under similar conditions

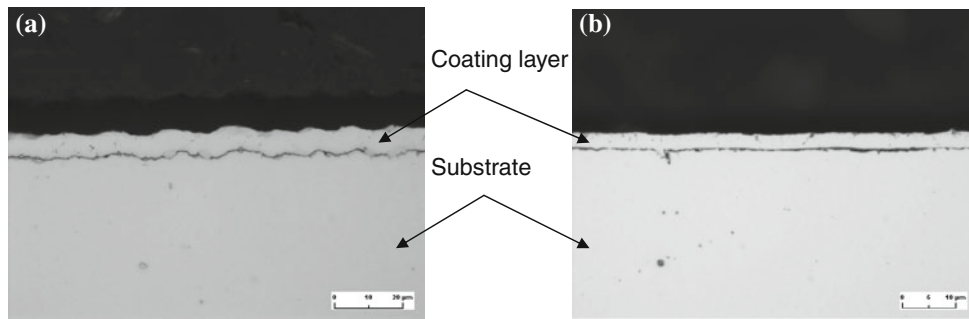


Fig. 6: Metallographic cross sections for two AZ-31 substrates, coated by pure Al layer—MS ion etching after different mechanical surface pretreatments: (a) rough surface (sand-blasted); (b) smooth surface (mirror-like polished)

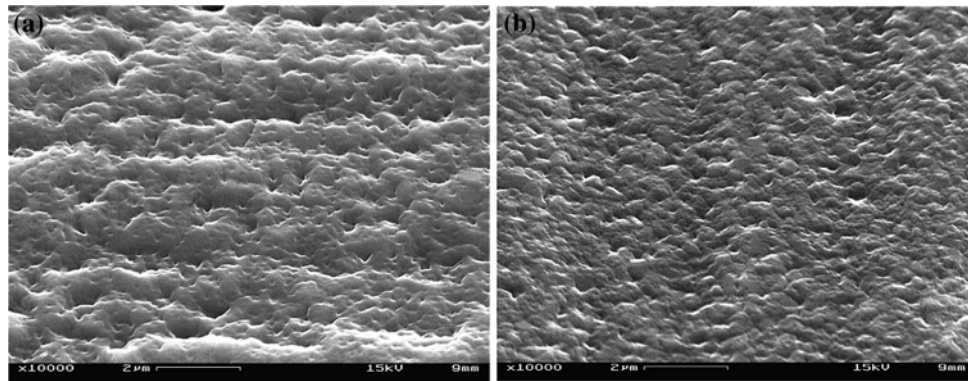


Fig. 7: Al coat surface morphology on Mg AZ 31 obtained by coating: (a) with plasma activation; (b) without plasma activation

indicated by the photomicrographs in Fig. 6 of the cross-sections of coated substrates in the case of a rough surface (sand-blasting) and a smooth surface (mirror-like). The results are in agreement with previous work on different substrate and target materials.²⁰

The deposited coat morphology was found to be affected by plasma activation. This is demonstrated by comparing two samples under the same conditions with and without plasma activation. Figure 7 indicates that although the morphology was similar in both cases, it is coarser in the case of plasma activation. This can be attributed to the high homologous temperature (substrate temperature/melting temperature of coating material) in the case of plasma activation¹⁷ due to the higher substrate temperature (Fig. 2). The reference reported that plasma activation enhances coat efficiency by increasing the substrate temperature, and that the coat tends to be dense and compact without any gaps or columnar structure.

Diffusion at the substrate interface

Diffusion at the interface between the Al coat and AZ 31 substrate was studied by GDOES analysis. In the

case of samples prepared without plasma activation and/or applying high substrate speeds, where substrate temperature rise was low, no diffusion of Al or Mg was observed.

In the case of samples using pure Al as target material, with plasma activation, and using the lowest substrate speeds between 1 and 1.5 cm/s, diffusion was enhanced due to substrate temperature reaching high values above 300°C. In a sample coated under these conditions, three deposition passes were made in order to have a layer thickness of 8 µm instead of 2.5 µm obtained by single pass. In this case, diffusion occurred between the substrate surface and coat layer, as indicated by a DOES test (see Fig. 8). The figure shows the variation of Al and Mg elements across coated sample cross sections, starting from the coating surface (0 depth) toward the Mg substrate: Mg diffused into the Al coat layer. At the interface (8 µm depth), the composition was around 10% Al and 90% Mg. In this case, formation of Al₁₇Mg₁₂ intermetallic phase was deduced from EDX analysis (see Fig. 9). Similar behavior was reported by I. Shigematsu et al.,²⁰ who applied diffusion coating on AZ91D using Al powder with heat treatment at 450°C for 1 h. This resulted in diffusion and formation of γ Al₂Mg₇ intermetallic phase.

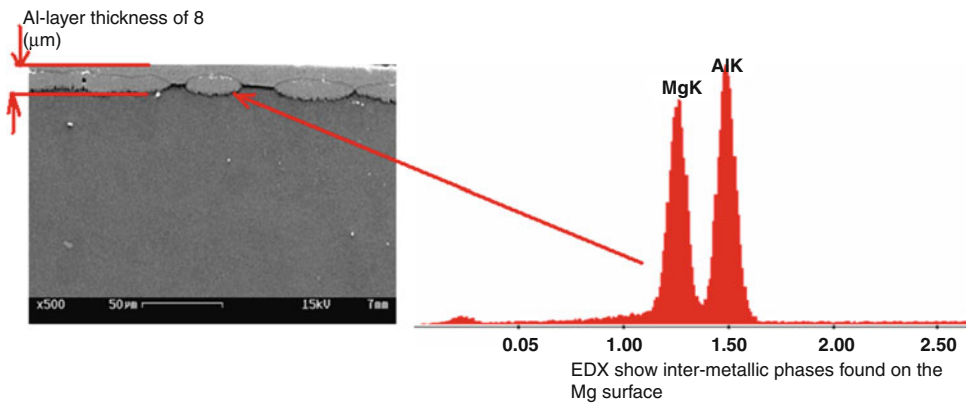


Fig. 8: Diffusion between the coating material (pure Al) and Az 31 substrate surfaces for specimens coated with plasma activation, using a low substrate speed of 1.5 cm/s given three coating passes

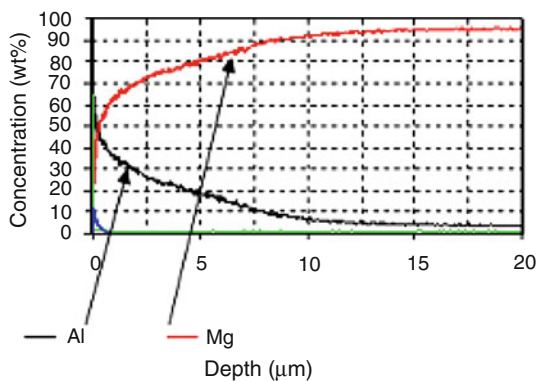


Fig. 9: EDX analysis for the diffusion zone on the AZ31 substrate surface for the sample in Fig. 8

Adhesion-bending test

Adhesion of the coating layer to the substrate surface was also tested by bending specimens 60 mm long × 20 mm in width cut from the coated substrates, and then using the tape test. Before bending, the tape was

adhered along the specimen. Bending was then done so that the coated surface with the tape was facing the die anvil. After bending, the tape was removed and examined microscopically while lying on a glass strip.

Figure 10 illustrates the bending test (Fig. 10a) and the results on three samples with different mechanical and ion-etching treatments; namely rough (sand-blast) followed by GD, polished (grade 600) followed by GD, and mirror-like polished followed by MS ion-etching (Fig. 10b). These samples were coated using MS without plasma activation.

Figure 11 indicates that in the case of GD ion etching, a partial removal of the coating layer was observed on the rough specimen while a complete removal was observed on the polished specimen. The results indicate poor adhesion in the case of coating after GD etching and partial adhesion on the rough substrate surface, which is attributed to mechanical interlocking.

In the third specimen, where MS ion etching was applied after mirror-like polishing, the coating layer was completely adhered without any coat removal. This is due to diffusion between the coat material and the substrate (see Fig. 11).

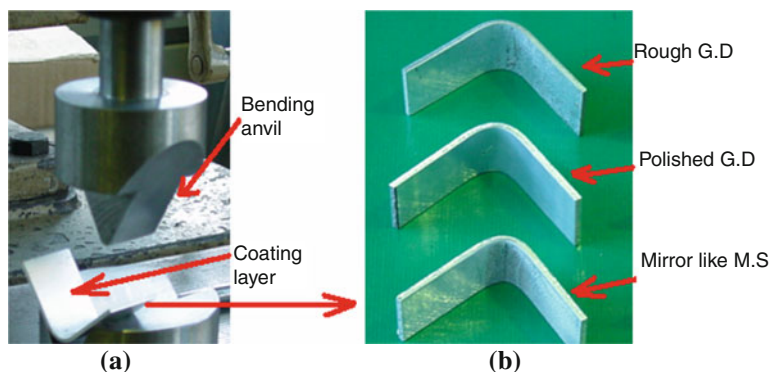


Fig. 10: Bending test applied to samples with different surface preparations, coated with pure Al coatings: conditions: (a) die and specimen location; (b) samples after bending

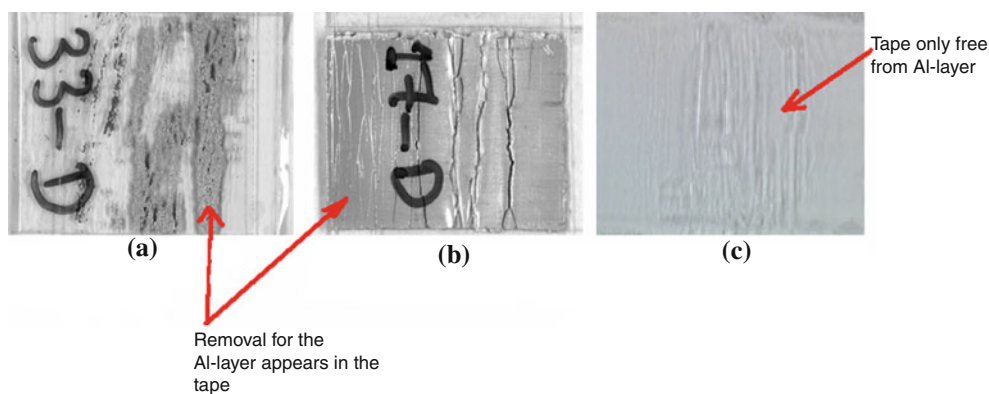


Fig. 11: Tape test results after bending for three samples coated with pure Al: (a) GD etching on rough surface; (b) GD etching on polished surface; (c) MS etching on mirror-like polished surface

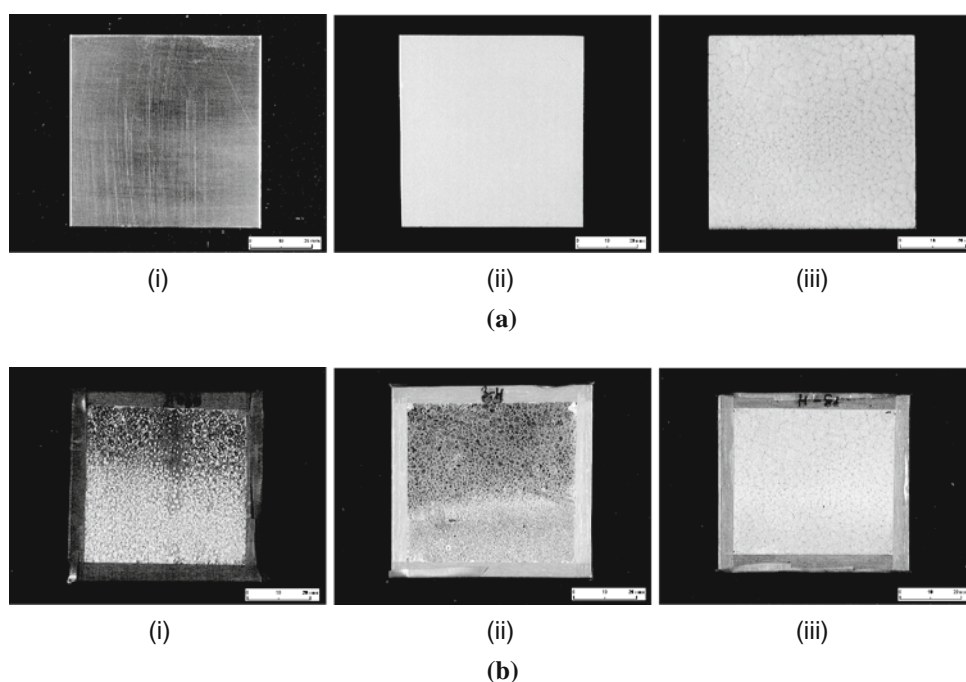


Fig. 12: Surface appearance before (a) and after (b) humidity test for Mg AZ 31 substrates: (i) no coat, (ii) pure Al coat with no diffusion, and (iii) pure Al coat with diffusion

Humidity test

Coating surface appearance, after a standard humidity test at 40°C for 48 h, is shown in Fig. 12 for specimens coated under different conditions. The figure shows that the uncoated sample was subjected to severe corrosion, as indicated by the high density white pits on the surface.

The results in Fig. 12 show that for the coated samples, the diffusion at the interface affects the corrosion resistance. This is indicated by the color change to dark gray due to corrosion products for the Al coating with no diffusion at the interface (see Fig. 12b-ii), while no corrosion products are found

where diffusion occurred in the Al-coated sample (see Fig. 12b-iii). The literature^{18,20} states that formation of intermetallic phases at the interface between substrate surface and coating layer is corrosion resistant and beneficial. A recent work by Wu²¹ highlights polarization tests carried out on samples coated with multiple Al layers, indicated that an Al coating could improve the corrosion resistance of Mg AZ 31 in a 3.5 wt% NaCl solution.

In general, the occurrence of galvanic corrosion between the noble Al and the active Mg alloy substrate should be prevented. For this purpose, the presence of the intermetallic layer on the Mg surface may help retardation of such galvanic corrosion.

Conclusions

The following conclusions can be drawn from this work:

1. For coatings of Mg AZ 31 substrate, the optimum surface preparation includes sand-blasting and polishing to a mirror-like surface, ultrasonic etching in a solution of sodium carbonate and sodium hydroxide, and then MS ion etching.
2. During ion etching, the substrate temperature increased to maximums between 140 and 180°C, depending on the surface pretreatment applied and ion etching technique used.
3. During PVD coating, a substrate temperature increase occurred, which varied inversely with the substrate speed. Plasma activation and/or coatings with pure Al resulted in a higher temperature increase. The highest substrate temperature of 375°C was measured on an Al coating applying plasma activation at a substrate speed of 1.5 cm/s.
4. Coating layer thickness varied similarly to substrate speed. Plasma activation resulted in a thinner coat with finer morphology. While coating with pure Al resulted in a thick layer reaching more than 6 µm, the Al–12.6% Si coat did not exceed 2 µm.
5. Diffusion of Al and Mg elements across the coating–substrate interface occurred at substrate temperatures above 300°C, and intermetallic phases were formed.
6. Good adhesion was achieved between the substrate surface and coating layer, and the coated surface indicated good resistance against humidity for coatings with Al where diffusion took place.

Acknowledgments The authors acknowledge Dr. Christoph Metzner and the cooperation by the Fraunhofer Institute for Electron Beam and Plasma Technology (FEP) in Dresden, Germany where the experimental work was conducted.

References

1. Landkof, B. "Magnesium Applications in Aerospace and Electronic Industries." In: Kainer, KU (ed.), *Proceedings of Magnesium Alloys and their Applications*, pp. 168–172. Wiley VCH Verlag, Weinheim (2000)
2. Sharma, AK, Uma Rani, R, Giri, K, "Studies on Anodization of Magnesium Alloy for Thermal Control Applications." *Met. Finish.*, **95** (3) 43–46, 48–51 (1997)
3. Sharma, AK, Suresh, MR, Bhojraj, H, Narayanamurthy, H, Sahu, SP, "Electroless Nickel Plating on Magnesium Alloy." *Met. Finish.*, **96** 10–18 (1998)
4. El Mahallawy, N, Palkowski, H, Shoeib, M, Maamoun, M, "Electro and Electroless Coating of Magnesium AZ31 Sheets: A Comparative Study." *Steel Grips*, **2** (2) 130–139 (2004)
5. El Mahallawy, NA, Palkowski, H, Shoeib, M, Maamoun, MA, Neubert, V, Bakkar, A, "Corrosion Protection of Mg Alloy by Nanostructure Deposits of Ni-P by Electroless Technique." *Steel Grips*, **4** (3) 212–216 (2006)

6. El Mahallawy, N, Bakkar, A, Shoeib, M, Palkowski, H, Neubert, V, "Electroless Ni-P Coating of Different Magnesium Alloys." *Surf. Coat. Technol.*, **202** (21) 5151–5157 (2008)
7. Yamamoto, A, Watanabe, A, Sugahara, K, Tsubakino, H, Fukumoto, S, "Improvement of Corrosion Resistance of Magnesium Alloys by Vapour Deposition." *Scr. Mater.*, **44** 1039–1042 (2001)
8. Yamamoto, A, Tsubakino, H, "A New Technique for Surface Modification in Magnesium Alloys by Applying Magnesium Oxide Coating." *Mater. Sci. Forum*, **419–422** 903–908 (2003)
9. Langefeld, S, Jonschker, G, Schmidt, H, "Neue Sol-Gel-Beschichtungen als Korrosions- und Verschleißschutz für NE-Metalle: New Sol-Gel Based Coatings as Corrosion- and Wear-Protection on Non-Ferrous Metals." *Materialwissenschaft und Werkstofftechnik*, **29** 23–29 (1998)
10. Weisheit, A, Lenz, U, Mordike, B, "Thermal Spraying on the Magnesium Alloys AZ91." *Metallurgica*, **51** (9) 470–474 (1997)
11. Tsubakino, A, Yamamoto, A, Watanabe, A, Fukumoto, S, "Coating on Rugged Surfaces of Magnesium Alloy with High-Purity Magnesium Film." *Proc. Int. Congress on Advanced Materials, their Processes and Applications*, Materials Week 2001, Munchen, 2001, pp. 1–6
12. Gray, JE, Luan, B, "Protective Coatings on Magnesium and Its Alloys—A Critical Review." *J. Alloys Compd.*, **336** 88–113 (2002)
13. El-Mahallawy, N, "Surface Treatment of Magnesium Alloys by Electroless Ni-P Technique with Emphasis on Zinc Pre-Treatment: A Review." In: El-Mahallawy N, Zhang, M (eds.), *Progress in Surface Treatment*, vol. 384, pp. 241–262. Key Engineering Materials, Trans Tech Publications (2008)
14. Bakkar, A, Galun, R, Neubert, V, "Microstructural Characterization and Corrosion Behaviour of Laser Cladded Al–12Si Alloy onto Magnesium AS41/Carbon Fibre Composite." *Mater. Sci. Technol.*, **22** (3) 353–362 (2006)
15. Chiu, LH, Lin, HA, Chen, CC, Yang, CF, Chang, CH, Wu, JC, "Effect of Aluminium Coatings on Corrosion Properties of AZ31 Magnesium Alloy." *Mater. Sci. Forum*, **419** (422) 909–914 (2003)
16. Kainer, U, Horst, N, "Thermal Spraying of Magnesium Alloys for Corrosion and Wear Protection Magnesium." In: Kainer, KU (ed.), *Proceedings of the 6th International Conference on Magnesium Alloys and their Applications*, pp. 860–868, DGM/Wiley-VCH Verlag GmbH (2004)
17. Metzner, C, Roegner, F, Heiness, J, Scheffel, B, "PVD Coating of Metallic Sheets and Strips." *Steel Grips*, **2** (2) 124–129 (2004)
18. Hoche, H, Allebrandt, D, Scheerer, H, Broszeit, E, Berger, C, "Design of Wear and Corrosion Resistant PVD-Coatings for Magnesium Alloys." *J. Maetrialwissenschaft und Werkstofftechnik*, **38** 365–371 (2007)
19. Hoche, H, Scheerer, H, Fritsche, R, Thissen, A, Flege, S, Broszeit, E, Berger, C, Ortner, H-M, Jaegermann, W, "Untersuchung des Sputter-Ätzens auf die Eigenschaften von PVD-CrN-Hartstoffschichten auf Magnesium AZ91hp." *J. Maetrialwissenschaft und Werkstofftechnik*, **33** 132–141 (2002)
20. Shigematsu, I, Nakamura, M, Saitou, N, Shimojima, K, "Surface Treatment of AZ91D Magnesium Alloy by Aluminum Diffusion Coating." *J. Mater. Sci. Lett.*, **19** 473–475 (2000)
21. Wu, G, "Fabrication of Al and Al/Ti Coatings on Magnesium Alloy by Sputtering." *J. Mater. Lett.*, **61** 3815–3817 (2007)